ISBN: 978-3-95450-201-1 doi:10.18429/JACoW-IBIC2018-WEPB12

DESIGN AND IMPLEMENTATION OF NON-INVASIVE PROFILE MONITORS FOR THE ESS LEBT

C.A. Thomas*, T. Grandsaert, H. Kocevar,
O. Midttun, N. Milas, R. Miyamoto, T. Shea,
European Spallation Source ERIC, Lund, Sweden

Abstract

Non-invasive Profile Monitors are designed and distributed along the ESS Linac. In the Low Energy Beam Transport (LEBT), a specific one has been designed to be primarily a beam position monitor. Its main requirement is to measure the beam position with 100 µm accuracy, and in addition it provides the beam profile and size. This performance have been shown to be possible and remains to be demonstrated experimentally. The instrument is also potentially capable of measuring the angle of the beam and its divergence. In this paper we will study the accuracy of such a measurement as function of the instrument image quality.

INTRODUCTION

Non-invasive Profile Monitors [1–3] (NPMs) have been designed at European Spallation Source for the measurement of the beam profile at high power [4]. They are distributed from the LEBT to the last section before the target. We call NPM a transverse profile monitor based on the interaction of the residual gas with the beam of charged particles. There are two principle which the NPMs are based on. One is performing an image of the beam induced gas fluorescence [1], and the other is performing a profile of the beam induced gas ionisation [3].

However, in the LEBT, the main role of the NPM is to measure the position of the beam with respect to the reference beam axis [5]. The required position accuracy is shown to be better than 50 µm, and it is assured by the alignment of the optical axis of the NPM in the general coordinate system in which the whole accelerator is defined. The measurement principle the NPM for the LEBT is based on imaging the gas fluorescence excited by the proton beam. The interaction of the beam with the vacuum residual gas has a same probability along the particle trajectory. Therefore, the fluorescence emission is uniform along the particle path. When projected on the image plane by an optic assembly, the image represents the trajectory of the particle, projected along the optical axis. As a result, the image from the NPM represents the beam profile along the beam trajectory, and projected along one of the transverse axis. Thus, it contains information on the beam position and angle, the size and divergence. Measurement on the image may retrieve this information, and it could be used for beam tuning applications.

In the following we will show how we model an NPM image, using beam parameters, and how the retrieval of these parameters from image processing and analysis can be affected by the image quality.

BEAM PROPERTIES FROM NPM IMAGE

A typical NPM image can be modeled taking into account the beam parameters, the optics parameters and the noise of the camera. Such an image can be seen in Fig. 1.

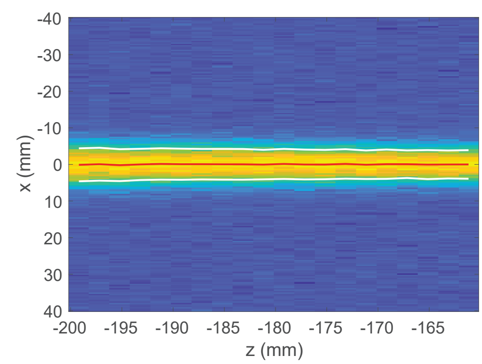

Figure 1: Model of an NPM image with ESS LEBT beam parameters. The white lines represents the beam size along the trajectory, and the red line the centre of mass, as retrieved by a Gaussian fitting algotrithm. SNR = 20.

To produce this image, we have used the beam transport model of the LEBT. The transport equations are given:

$$\beta_z = \beta_0 - 2\alpha_0 z + \gamma_0 z.^2 \quad (1)$$
$$\alpha_z = \alpha_0 - \gamma_0 z \quad (2)$$
$$\gamma_z = (1 + \alpha_z^2)/\beta_z \quad (3)$$
$$\sigma_x = \sqrt{\beta_z \varepsilon} \quad (4)$$
$$\sigma_x' = \sqrt{\varepsilon \gamma_z} \quad (5)$$
$$c_x = a_1 z + a_0 \quad (6)$$

in which z is the beam longitudinal propagation coordinate; $\varepsilon = 16.8 \cdot 10^{-6}$ m.rad, the beam geometrical emittance; β_z, α_z, γ_z, the beam Twiss parameters at the coordinate z; $\beta_0 = 0.11$ m, $\alpha_0 = 1.02$, $\gamma_0 = 18.54$ m^{-1}, the Twiss parameter at the beamwaist at the exit of the LEBT; σ_x the beam size, and σ_x' the beam divergence; c_x is the beam centroid; a_i are the coefficient for the first order polynomial describing the kick angle of the beam.

Using Eqs. 5 and 6, one can compute the beam profile along the propagation axis, assuming for instance a Gaussian distribution.

* cyrille.thomas@esss.se

ISBN: 978-3-95450-201-1 doi:10.18429/JACoW-IBIC2018-WEPB12

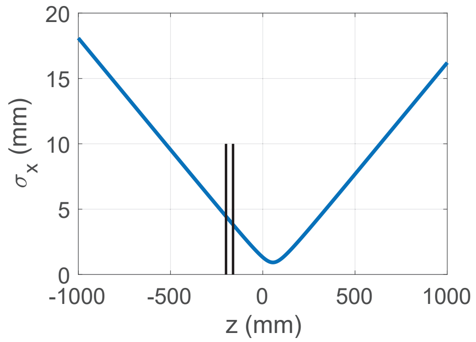

Figure 2: Beam Size along the path using Eqs. 1 to 5. The vertical lines show the field of view of the NPM.

The coodinates of one of the NPMs in the LEBT is at is $z = -180$ mm from the beamwaist in the LEBT extraction cone. The result of the calculation of the beam size along the path is shown in Fig. 2.

To generate the image shown in Fig. 1, we have generated Gaussian profiles, in which the r.m.s. size is given by Eq. 4 and the centre of mass is given by Eq. 6.

IMAGE QUALITY AND MEASUREMENT UNCERTAINTY

The quality of the measurement of the beam parameters can be affected by several aspects from the instrument. In first place, the beam size and position can be affected by the resolution of the system. The position accuracy depends on the quality of the optical axis aligment; the precision of the position depends on the accuracy in knowing the image magnification. This has been reported in [5]. We will not discuss it in this paper.

All cameras produce an image, in which the light intensity is digitized. The image has an offset background, and the intensity is linear over a range defined by the digital scale. The linearity of the sensor response is critical to retrieve the beam profile. This can be measured and is given by camera manufacturers in the EMVA 1288[1] standard associated report. Most cameras, whether CCD or CMOS are relatively linear within better than 1%, which guarantees the profiles to be proportional to the beam profiles.

The other important camera property that may be critical is the total noise of the sensor. In order to model the noise, we generated images with added random noise, uniformely distributed over the image.

The expression to generate the image is then given by:

$$Im\,(x,z) = N\text{randn}(x,z) + I_0 e^{-\frac{(x-c_x(z))^2}{2\sigma_x(z)^2}} \qquad (7)$$

This describes a Gaussian distribution in the axis x, which has a r.m.s size, σ_x and centre position, c_x, depending on the position z. The noise is generated using a random normal distribution, with an arbitrary offset equal to 50 and a typical width of 1. This noise distribution can model many ones as measured on cameras like for instance the one selected for the NPM in the LEBT. The intensity scale of the image ranges over 12 bits.

[1] https://www.emva.org/standards-technology/emva-1288/

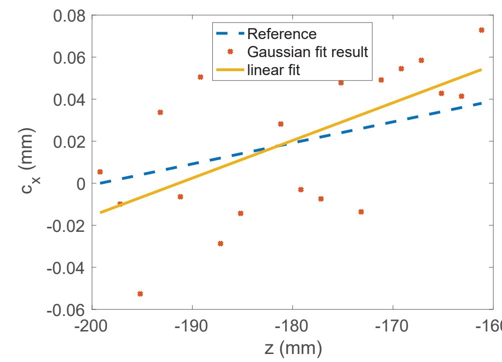

Figure 3: Kick angle of the beam as measured on the Fig. 1 generated image.

In order to model the performance of the measurement of the beam size and centre of mass along the beam path we use Eq. 7, varying the intensity I_0 in a range from 1 to 1000 counts. The distribution of the noise is kept at $\sigma_{\text{noise}} = 1$ counts. This defines the signal to noise ratio: $\text{SNR} = I_0/\sigma_{\text{noise}}$.

Angle Measurement Uncertainty

The beam is modeled so that it receives a kick and its centre moves along a trajectory defined by the kick angle. In the simulation, the kick angle varies from -26mrad to 26mrad. For each selected kick angle, 1000 images are produced with newly generated noise.

For each image, as shown in Fig. 1, a Gaussian fit is performed over 20 lines along 40 mm of propagation axis. The result of the fit gives the centre and size of the beam along the trajectory z.

A linear polynomial fit is performed on the centres to find out the kick angle. Figure 3 shows the beam centre trajectory as measured by the Gaussian fit. It is compared to the reference beam trajectory. The line generated by the linear polynomial fitting the centre trajectory is also shown. The SNR on the image is 50. The statistical angular measurement error is $\Delta\theta \approx 0.5$ mrad.

The result of the simulation for a given SNR can be seen in Fig. 4. Here the SNR=100. The left axis shows the mean value of the measured angle, plotted against the reference kick angle. The error between the mean measured angle and the reference is less than 0.1% . On the right axis, the standard deviation over 1000 measured kick angles is reported. This corresponds to the statistical error of the measurement. The average error in this case is $\Delta\theta = 0.26$ mrad.

Figure 5 summarises the results obtained for the kick angle statistical error vs. SNR. The statistical error in this particular case, where the beam size corresponds to ≈ 10 pixels, seems to be less than 1 mrad for SNR larger than 25.

ISBN: 978-3-95450-201-1 doi:10.18429/JACoW-IBIC2018-WEPB12

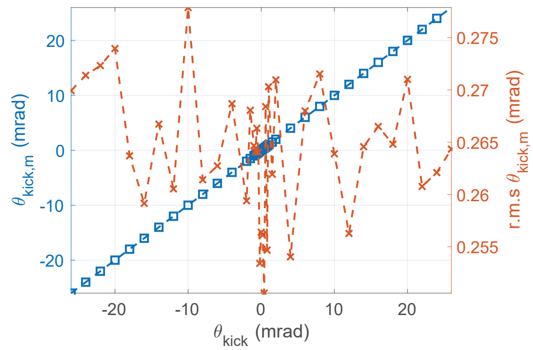

Figure 4: Kick angle and error on a measurement for an image with SNR = 100.

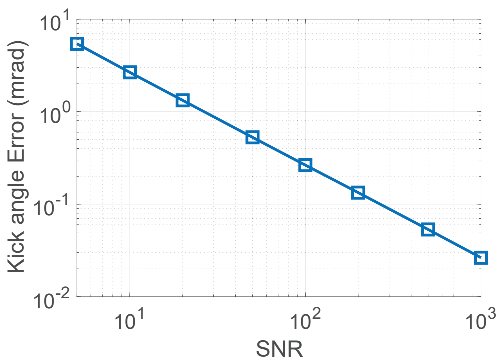

Figure 5: Kick angle statistical error as function of the SNR.

Beam Size Trajectory Uncertainty

The beam size can be measured along the trajectory. The beam size statitical uncertainty is computed by the standart deviation of the set of measurements compared to the reference beam size. The Fig. 6 shows the standard deviation of the measured beam size, $\Delta_{\sigma_x} = \left\langle \left(\sigma_x - \sigma_{x,ref}\right)^2 \right\rangle^{\frac{1}{2}} / \sigma_{x,ref}$, relative to the reference beam size, $\sigma_{x,ref}$, and as function of the SNR. The statistical error on the measurement of the beam size is smaller than 3% for SNR larger than 10.

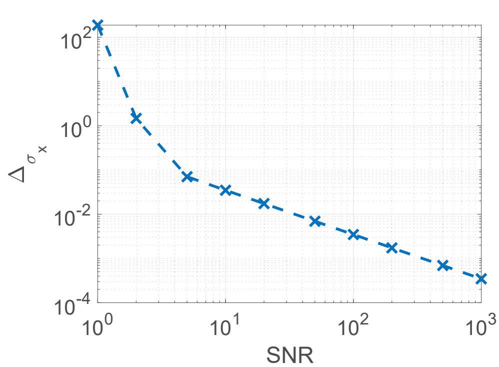

Figure 6: Standard deviation of the beam size measurement as function of the SNR and relative to the beam size.

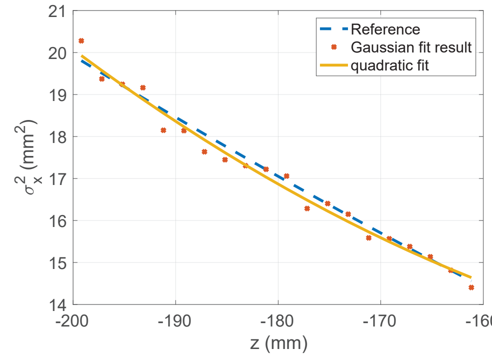

Figure 7: Square of the beam size as measured on the Fig. 1 generated image.

The beam size square is expected to be a quadratic function of z, as defined by Eqs. 1 and 4. The Gaussian variance values trajectory of each image is fitted by a second order polynomial, expressed as $\sigma_x^2 = a_0 + a_1 z + a_2 z^2$. The coefficients a_i given by the result of the fit can be compared to the reference as given by Eqs. 1 and 4.

An example of such a fit is shown in the Fig. 7. It presents the beam size square trajectory as fitted by a Gaussian, and compared to the reference. The fitting second order polynomial is also shown.

The mean values of the quadratic polynomial coefficients is shown in the Fig. 8 as function of the SNR. The deviation of the coefficients from their reference, $\varepsilon\beta_0$, $\varepsilon\alpha_0$ and $\varepsilon\gamma_0$, is rather large for values of the SNR smaller than 5. However, for SNR larger than 5, the relative error is less than 5%, and for SNR larger than 20 it is less than 0.5%

The standard deviation of the quadratic coefficients measurement is shown in the Fig. 9. The plot shows the standard deviation over the set of measurements, $\langle a_i^2 \rangle^{1/2}$, divided by the mean values, $\langle a_i \rangle$. Relative spreads much smaller than unity can be seen for unsignificant noise figure, typically SNR>500. The noise has a strong impact on the variance of the measurement of the quadratic fit coefficient. This is not a surprise. The position of the NPM is far from the beam waist, where the parabola has a very small curvature. Thus, statistical deviation in the beam size measurement that is larger than the curvature impacts strongly the result of the quadratic fit.

CONCLUDING REMARKS

The measurement of the images performed by an NPM based on residual gas fluorescence could be used to measure beam position and angle. The angle of the beam can be measured with high precision. In the example studied, for SNR>25, the statistical error is expected to be less than 1 mrad. The accuracy of the measurement also depends on the fiduscialisation of the NPM. As shown in [5] the accuracy of the position can be better than 50 µm.

ISBN: 978-3-95450-201-1 doi:10.18429/JACoW-IBIC2018-WEPB12

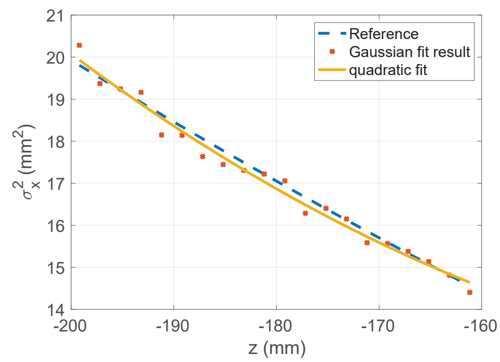

Figure 8: Mean values of the quadratic fit coefficients. Each curves is compared to their reference, as given by the Eq. 1 and 4.

.

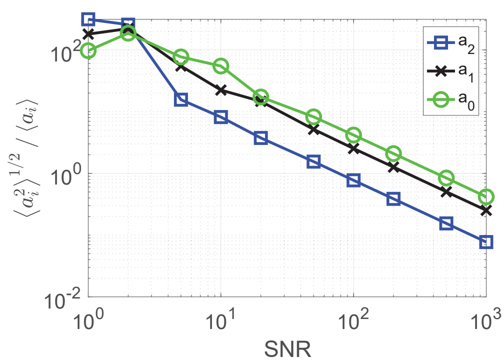

Figure 9: Relative error for the fit of the beam size square.

The beam size can also be retrieved from measurement on the image. The presicision of the measurement is better than 3% for SNR larger than 10.

The beam size square trajectory can be measured on the NPM image. However, at the location of the second NPM in the LEBT studied here, the uncertainty on the parabolic fit is highly dependent on the noise in the image. With SNR larger than 500, the fit return the parabola coefficients within the same order of magnitude. But the average value fall within few percents for SNR larger than 5.

The measurement of the beam size trajectory could also provide more information on the lattice. The Twiss parameters could be retrieved in principle, but it is not discussed in this paper. The measurement however can provide some qualitative information during the commissioning of the accelerator.

The verification of the measurments of the beam and beam size trajectories using an NPM is expected to be done while commissioning of the NPM for the LEBT.

REFERENCES

[1] D.P. Sandoval. Fluorescence-Based Video Profile Beam Diagnostics: Theory and Experimence. In *BIW*, Santa Fe, New Mexico, USA, 1993.

[2] P Forck and A Bank. Residual Gas Fluorescence for Profile Measurements at the GSI UNILAC. In *EPAC*, 2002.

[3] W. H. DeLuca. Beam detection using residual gas ionization. *IEEE Transactions on Nuclear Science*, 16(3):813–822, June 1969.

[4] B Cheymol, C Bohme, A Jansson, H Hassanzadegan, I Dolenc Kittelmann, T Shea, and L Tchelidze. Overview of the european spallation source warm linac beam instrumentation. In *Proc. of International Beam Instrumentation Conference (IBIC'13)*, International Beam Instrumentation Conference, pages 346–348, Geneva, Switzerland, Sept. 2013. JACoW.

[5] C.A. Thomas et al. Design and Implementation of Non-Invasive Profile Monitors for the ESS LEBT. In *Proc. of International Beam Instrumentation Conference (IBIC'16), Barcelona, Spain, Sept. 13-18, 2016*, number 5 in International Beam Instrumentation Conference, pages 552–555, Geneva, Switzerland, Feb. 2017. JACoW. doi:10.18429/JACoW-IBIC2016-TUPG80.